Proceedings of the International Symposium on Room Acoustics, ISRA 2010

29-31 August 2010, Melbourne, Australia

Application of analytic sweep segments in room acoustic measurements

Csaba Huszty (1), Sakae Yokoyama (2) and Shinichi Sakamoto (2)

(1) Graduate School, The University of Tokyo
(2) Institute of Industrial Science, The University of Tokyo
Ce 401 4-6-1 Komaba, Meguro-ku, Tokyo, 153-8505, Japan

PACS: 43.20.Ye, 43.58.Gn, 43.55.Mc

ABSTRACT

Room acoustic measurements employing indirect signals to obtain room impulse responses are widely used nowadays, particularly swept sine signals. In this paper, application of a general method creating excitation signals solely in time-domain with sigmoid, monomial power function and generalized exponential modulation functions are presented. By using such signals it is possible to match different optimization criteria such as customizing the SNR-frequency function of the resulting room impulse response and obtain useful results in a wider frequency region where excitation signal is present. Theoretical and practical aspects are presented with measurement results and total harmonic distortion (THD) response analysis.

INTRODUCTION

Room acoustic measurements nowadays often employ indirect measurement methods, such as sine sweeps. Sine sweeps have many advantageous properties over random or pseudo-random measurements and over direct impulsive measurements. Generation of sine sweeps is divided into two major methods, one in the frequency domain (TSP / time-stretched pulse method [1,2]) and one in the time-domain [3,4]. Frequency-domain generation results in an imperfect signal envelope while time-domain generation an imperfect frequency response assuming that the length of the signal is finite.

In room acoustic measurements probably the most widely used signals are the pink and white sweeps but even with these signals it is often difficult to obtain an acceptable SNR in the low frequency region. Usually, the SNR function versus frequency in the measured impulse response is not flat which suggests the background noise in the room and of the equipment together is usually neither white nor pink (assuming a transparent measurement system).

In the frequency domain, there are already approaches to synthesize background-noise matched sine sweeps [5,6]. However, a flexible and easy to use time-domain method has not yet been suggested as the generating time-domain formulas were hitherto unavailable. Also, matching the sweep rate to the background noise will not always produce flat SNR functions in practice as the measurement equipment, particularly the loudspeaker (having a non-flat frequency response) may attenuate various, especially low frequencies. Therefore, in some cases, not a flat frequency response but focusing to a particular frequency range may be important, thus, flexibility is required.

In this paper we propose and verify the application of segmented, phase aligned time-domain signal generation using customizable short sweeplets.

ANALYTIC SWEEP SEGMENTS

Segmented signal generation

A sine sweep containing segments of sweeplets can be written as the concatenation of various phase functions:

$$s(t) = A \cdot \sin([\Phi_1(t), \ldots, \Phi_N(t)]) = A \cdot \sin\Phi_c \quad (1)$$

During concatenation, phase alignment should be guaranteed, which is an easily solvable numeric problem if the phase functions are monotonic, for example in an upwards sweep. An example of phase alignment of two sweep signal segments is shown in Fig. 1.

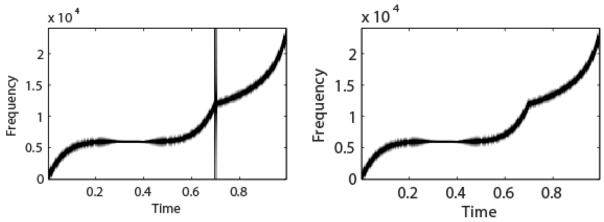

Figure 1. Spectrograms of a sine sweep consisting of 2 segments concatenated. Left: unaligned. Right: phase aligned.The audible click (vertical line in the left figure) is mitigated if phase-alignment is conducted.

Sweeplet generation

In the following we present three time-domain sweeplet signals that can be parameterized according to various optimization criteria, such as background noise matching.

The ‘color sweeplet’, capable of matching background noises having a power spectra proportional to $1/f^{\beta}$ with $\beta \in \mathbb{R}$ can be generated with the time-domain function

$$s(t)_{\mathrm{c}} = A\sin\left(\frac{T\,(\omega_1-d)}{\alpha\,\gamma}\left(\left(\frac{t}{T}\,\alpha+1\right)^{\gamma}-1\right)+d\,t\right) \quad (2)$$

where

$$\alpha = \left(\frac{\omega_1-d}{\omega_2-d}\right)^{\beta-1}-1 \quad \text{and} \quad \gamma = \frac{\beta-2}{\beta-1} \quad (3)$$

In (2), T is the length of the sweep signal, t is the momentary time, A is the amplitude of the sweep and ω_1 and ω_2 the starting and ending angular frequencies, respectively. d is a free parameter that can be chosen to bend the overall spectrum whose inclination is defined by β.

Such $1/f^{\beta}$ noises can be, for instance white ($\beta = 0$), pink ($\beta = 1$), red (or Brownian, $\beta = 2$) or other colored noises (Table 1).

Table 1. Noise colors

color	*magnitude shape [dB/octave]*	β
violet / purple	6	-2
blue / azure	3	-1
white	0	0
pink	-3	1
red (Brownian)	-6	2

It shall be noted that the formulation of (2) is such that only limits for the exponential and red sweeps exist, which can be written in closed form as:

$$\lim_{\beta\to1} s(t)_{\mathrm{c}} = A\sin\left(\frac{(\omega_1-d)\,T}{\ln\left(\frac{\omega_2-d}{\omega_1-d}\right)}\left[\mathrm{e}^{\frac{t}{T}\ln\left(\frac{\omega_2-d}{\omega_1-d}\right)}-1\right]+d\,t\right) \quad (4)$$

and

$$\lim_{\beta\to2} s(t)_{\mathrm{c}} = A\sin\left(\frac{(\omega_1-d)\,T}{\frac{\omega_1-d}{\omega_2-d}-1}\ln\left(\frac{t}{T}\left(\frac{\omega_1-d}{\omega_2-d}-1\right)+1\right)+d\,t\right) \quad (5)$$

respectively. By using parameter d different sweep shape customizations are possible (Fig. 2).

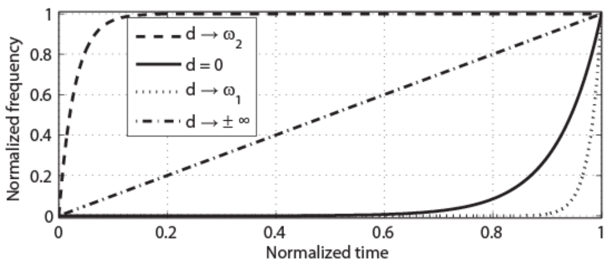

Figure 2. Different sweep rates of the generalized exponential sweeplet parameterized by d.

These color sweeplet signals have a monotonic spectrum either inclining or declining according to the values of d and β. However, de-focusing within a particular band is possible when the sweep is generated with the formula:

$$s(t)_{\mathrm{sigm}} = A\sin\left(d\,t+\frac{T\,(\varepsilon+1)\,(d-\omega_1)\ln\left(\frac{\theta(\varepsilon+1)}{\varepsilon(\theta+1)}\right)}{c+\ln(\zeta)}\right) \quad (6)$$

where $s(t)_{\mathrm{sigm}}$ is the 'sigmoid' sweep, in which for shorter notation

$$\varepsilon = \mathrm{e}^{-c}$$

$$\zeta = \frac{\omega_1-\omega_2-\varepsilon(\omega_1+d)}{\omega_2-d} \quad (7)$$

$$\theta = \exp\left(\frac{t\ln(\zeta)-Tc+ct}{T}\right)$$

are introduced. In this case

$$d > \omega_2 \quad \text{and} \quad c \geq 0 \quad (8)$$

yields real results. When $d \cong \omega_2$ is fixed and c increasing the sweeplet tends gradually from an S-shape to an ω_1 constant frequency signal. Such S-shape is a focus to the sides of the excitation band in the overall frequency response, thus forming a defocusing or notch sweeplet.

On the other hand, focusing at a particular frequency is possible using the 'monomial higher order power sweeplet' which can be generated by:

$$s(t)_{\mathrm{mp}} = A\sin\left(\frac{T\,(\omega_1-d)}{\eta\cdot c^{p}\,(p+1)}\left(\left(\frac{Tc+\eta t}{T}\right)^{q}-c^{q}\right)+d\,t\right) \quad (9)$$

where

$$\eta = \frac{\left(c^{p}\,(\omega_2-d)\right)^{\frac{1}{p}}}{\omega_1-d}-c \quad (10)$$

$$q = p+1$$

is introduced for shorter notation. The monomial higher order power sweep (using d) has parameter control features in common with the generalized red sweep when p approaches -1 since:

$$\lim_{p\to-1} s(t)_{\mathrm{mp}} = s(t)_{\mathrm{g.red}} \quad (11)$$

In order to obtain a real result, the monomial sweep's free parameter has to follow

$$d\!:\begin{cases}\omega_1 > d > \omega_2: & c^{p} > 0\\ \omega_1 < d < \omega_2: & c^{p} < 0\end{cases} \quad (12)$$

and frequency focusing is possible when

$$c < 0 \quad \text{and} \quad p = 2k+1 \quad \text{where} \quad k \in \mathbb{Z}^{+}. \quad (13)$$

By increasing k the focus can be set to last longer relative to T (Fig. 3).

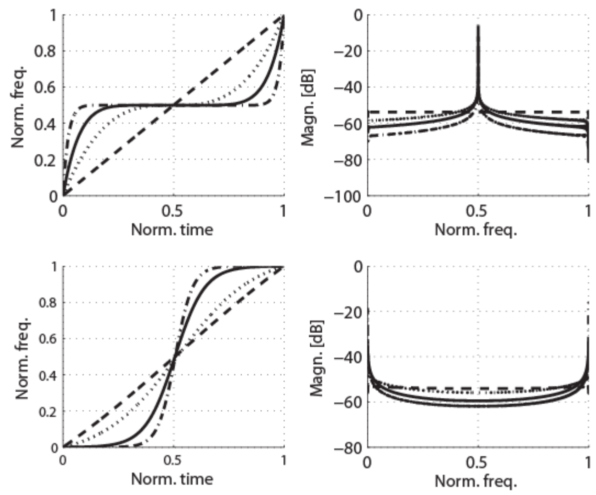

Figure 3. Frequency focus and notch with monomial and sigmoid sweeplets; left: spectrogram, right: spectrum. Top: monomial power sweeplet, $d = \omega_2/2$; dashed $p = 1$, dotted $p = 3$, solid $p = 7$, dotted dashed $p = 21$. Bottom: sigmoid sweeplet with dashed d and c jointly increasing.

INVERSE FILTER

Properties of the impulse response are prescribed by the inverse filter which compresses the source signal into an approximated impulse. The room can be treated as an infinite-input infinite-output model, which is usually simplified to a multiple-input multiple-output (MIMO) system where measurements are conducted at selected input-output pairs. Therefore, during the measurement a single input single output (SISO) system is considered.

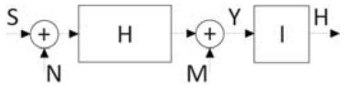

Figure 4. SISO model of room impulse response measurement

In order to obtain H (the Frequency Response Function, FRF), various FRF estimators were developed and used. In this present approach we use the H_1 no-input-noise FRF estimator

$$H_1(j\omega) = \frac{S_{SY}(j\omega)}{S_{SS}(j\omega)} \tag{14}$$

where $S_{SY}(j\omega)$ denotes the cross-spectrum of the noise-free input signal $S(j\omega)$ and the recorded noisy signal $Y(j\omega)$. If a single sweep is recorded and there is no averaging employed this can be reduced to

$$I(j\omega) = S^{-1}(j\omega). \tag{15}$$

In this case, it is required that full $[0..f_s/2]$ range is excited, otherwise $I(j\omega)$ should be multiplied with an appropriate bandpass filter, which is both frequency and time-wise compact and does not introduce too much time-smearing.

MEASUREMENT TIME AND PROCEDURE

During the measurements we create the sweeps according to a desired overall spectrum, which can be obtained for example by a short on-site measurement of the background noise. Once the target frequency response is available, it is cut into bands so that each band can be matched with a particular sweeplet. Next, the particular sweeplet is selected according to the spectrum shape of the target band and the free parameters (i.e. c, d, p or β) are set. Lastly, the sweeplet length ratios are selected so that they give the desired overall spectrum. Such length ratios are proportional to the ratios of the spectrum magnitudes of the segments.

In this present approach we employ linear convolution in the inverse filtering, thus a sweep signal is followed by the recording of silence or room noise. Long signals assume time invariance in the system for the full measurement time.

If the silence part is cropped or omitted, the resulting spectrogram will feature the room noise dynamically cut according to an inverse-sweep shape (Fig. 5) introducing misleading curvatures in te energy decay curve (EDC); therefore, length greater than the maximum decay time is preferred. Here in the example measurements we use the length $\boldsymbol{2T}$.

If averaging is used, the distances between the sweep signals can be shorter than T (even overlapping is possible), but such excitation signals are not considered in this present approach.

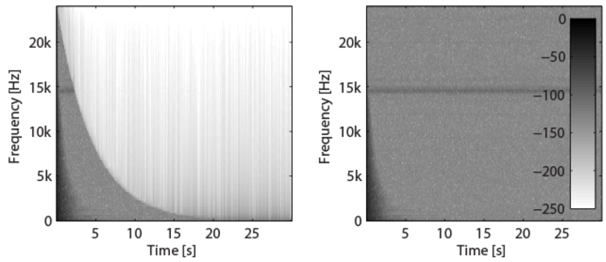

Figure 5. Measurement examples with a 30-second exponential sweep using measurement length T (left) and 2T (right). Colors denote magnitude in dBFS. Truncated signals (left) will introduce frequency-dependent double slope energy decay curves because the noise is truncated.

The procedure is as follows:

1. the desired sweep signal is synthesized in time-domain using concatenated sweeplet segments
2. the inverse filter of the whole sweep signal is calculated in the frequency domain
3. the T length sweep signal is excited into the system and the measurement signal is obtained; the measurement lasts longer than T to allow the decay process of the system to finish and in order to support linear convolution in the inverse filtering; for simplicity we use $2T$ measurement lengths
4. after the $2T$ long measurement signal is obtained, it is inverse filtered and the $2T$ long impulse response is cropped to length T.

EFFECTS OF NOISE AND HARMONIC DISTORTION

Real measurements often suffer from background noise and if loudspeakers are used harmonic distortion must be considered; therefore effects of these are briefly examined in this section.

Stationary noise

Stationary noise can enter the measurement system at points N and M (Fig. 4). In both cases, the noise of the impulse response will be similar, the only difference is that for N, the noise will be convolved with the impulse response, but otherwise, the inverse filter transforms them similarly. The measured impulse response consists of the noise-free impulse response and additional components due to the noise:

$$H_{meas} = H + \frac{HN+M}{S} \tag{16}$$

By increasing the signal length k times compared to its original, the achievable signal-noise ratio increases $10\lg k$ in dB since there is more energy in the signal. In theory, this is true without limit for any k, but in practice it is true usually only up to a certain case-by-case limit, due to possibly time invariance and inverse filter conditions. For example, if the sweep signal is only band-limited or if there is lengthy time-half-windowing applied in order to overcome turn-on transients, certain frequencies in the noise will not take part in the averaging process thus reducing the SNR gain.

We simulated a measurement scenario by employing different sweep lengths and a single measured background noise in a reverberation room. We used an inverse filter based on an idealistic, full-band sweep, therefore, all frequencies in the noise are processed by the inverse filter. When the time-half-window length was small compared to the sweep length (approximately 1000 times smaller in this example), the achieved SNR gain followed the idealistic measurement results, and both following the theoretic expectations (Fig. 6).

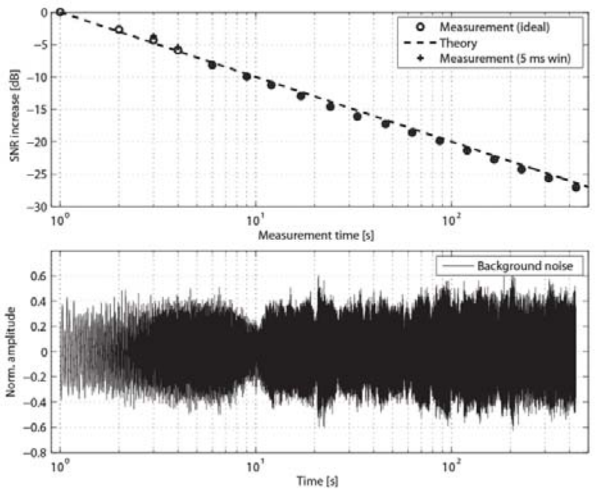

Figure 6. Theoretical and practical achievable SNR gain (top) based on measured background noise (bottom) transformed by inverse filters of sweeps of different length.

Transient noise

Since the inverse filter defines the transformation between two opposite signal shapes (the swept sine and the impulse), when transient (impulse-like) noises disturb the swept sine measurements, they will be transformed into reversed sweep shapes. In a sweep with increasing frequency, noise components above the actual frequency will be transformed so that their components will be located before the beginning of the baseband impulse response, therefore, the earlier in time a wideband transient noise occurs, the least perturbation it causes. Mitigation of these effects can be realized in practice for example by bandpass or lowpass filtering a small portion of the obtained measurement signal [9]. It is also possible to modify the inverse filter to match the transient noise. Neither approaches can be said to be generally correct for all practical cases.

Harmonic distortion

Membrane-based loudspeakers introduce harmonic distortion to the excitation signal. If the inverse filter is formulated according to undistorted perfect sweeps (uncompensated case), components due to harmonic distortion appear in the impulse response. These components have a dispersive impulse shape and can thus affect the whole impulse response. If the sweep is a pure exponential, the components compress into sub-band impulses, temporally separable from the baseband.

In case the harmonic distortion model of the particular speaker is available, measurements can be compensated by formulating the inverse filter according to a similarly distorted signal such that

$$S(j\omega) \coloneqq S_{dist}(j\omega). \tag{17}$$

This way, any kind of distorted full-band sweep can be transformed into a perfect impulse.

In the other, uncompensated case, the harmonic distortion components are most easily separable from the baseband impulse if they compress into one temporal position. Formally, this is achieved if the τ time difference of any distortion component from the baseband signal is time-independent [5, 8], which can be verified by solving (18) for τ, using the phase functions for each sweeplet:

$$N\frac{\mathrm{d}}{\mathrm{d}t}\Phi(t) = \frac{\mathrm{d}}{\mathrm{d}t}\Phi(t+\tau) \tag{18}$$

where for every $N > 2 \in \mathbb{Z}^+$, τ is the distance of the N-th harmonic from the baseband signal. For the color sweeplet the solution exists but too long to display. For the generalized exponential sweeplet the closed form can be simplified to:

$$\tau(t)_{exp} = \frac{T\ln\left(N\left(\frac{d-\omega_2}{d-\omega_1}\right)^{\frac{t}{T}} - \frac{d\,(N-1)}{d-\omega_1}\right)}{\ln\left(\frac{d-\omega_2}{d-\omega_1}\right)} - t \tag{19}$$

where it can be seen that independence of t can be achieved by setting $d = 0$ yielding the formula presented in [8].

$$\tau(t)_{exp}\big|_{d=0} = \frac{T\ln(N)}{\ln\left(\frac{\omega_2}{\omega_1}\right)} \tag{20}$$

For the sigmoid and monomial power sweeplet the solution is:

$$\tau(t)_{sigm} = \frac{T(c+\ln(\eta))}{c+\ln\left(\alpha^{\frac{T}{t}}\right)} \tag{21}$$

where

$$\eta = -\frac{\omega_1\,\delta\,\beta - d(\beta + Ne^{c}\alpha)}{e^{c}(d(N(1-\alpha)+\alpha+e^{c}) - \delta\,N\omega_1)} \tag{22}$$

$$\delta = 1 + e^{c}$$

$$\alpha = 1 - \frac{\delta(\omega_1 - \omega_2)}{-\omega_2 + d}$$

$$\beta = \alpha + e^{c}(1 - N)$$

and

$$\tau(t)_{mp} = \frac{T}{c-\gamma}\cdot\left(c - \left(\frac{dc^{p} - N(\chi(\omega_1 - d) + dc^{p})}{d-\omega_1}\right)^{\frac{1}{p}}\right) - t \tag{23}$$

where

$$\chi = \left(\frac{t\gamma - tc + cT}{T}\right)^{p} \tag{24}$$

$$\gamma = \left(\frac{c^{p}(d-\omega_2)}{d-\omega_1}\right)^{\frac{1}{p}}$$

In these cases the solutions are not independent of t. If an uncompensated inverse filter is used, time aliasing between the harmonic and baseband responses may appear if the system response has a considerable length compared to the sweep length. Even if the harmonics are compressing into the same time moment, enough time should be present between them so that their responses decay before the baseband sweep's given frequency is excited (assuming an upwards sweep). The measurement signal length should be chosen accordingly, using:

$$N\frac{\mathrm{d}}{\mathrm{d}t}\Phi(t) = (N-1)\frac{\mathrm{d}}{\mathrm{d}t}\Phi(t + R(\omega)) \tag{25}$$

where at each ω angular frequency $R(\omega)$ is the *a priori* known or assumed reverberation time. Since $\frac{\mathrm{d}}{\mathrm{d}t}\Phi(t) = \omega(t)$ can be evaluated analytically, the determination of the minimum measurement time is possible.

MEASUREMENT RESULTS

Observable background noise in rooms

During the several last years, various acoustic spaces in Hungary were measured with the exact same equipment. For this paper, 23 halls, including rehearsal rooms, scoring stages, concert halls of different sizes, churches, cathedrals and large natural caves were examined focusing on the observed background noise in the on-site recorded signals. Since the same equipment with the same setup was used everywhere we cannot easily conclude that other measurement scenarios will also follow the same pattern, still, it seems to be a common problem in room acoustics that high SNR at low frequencies cannot be easily obtained. This, as authors believe is not only due to the lack of excitation, but also due to the observable background noise spectra.

Results suggest that the overall observable background noise in a room, including the room background and equipment noise, is slightly more ‘warm’ even than red noise, suggesting that red sweeps match the room conditions better than the widely used exponential (pink) or linear (white) sweeps (Fig. 7).

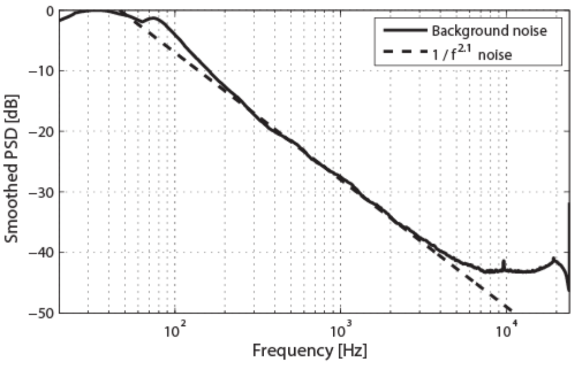

Figure 7. Average smoothed power spectral density of observed background noises (including equipment noise) in 23 different halls, using 2-second noise samples of 1933 different measurements (solid), and a robust linear regression fit (dashed) on the obtained result. $\beta = 2.1$ means that the background noise is similar to a red noise.

Test measurements with sweep customization

In this section some measurement examples are presented using the already present noises and additional artificial background noises in a reverberation room. In the first case, the artificial noise was a two-harmonic pure tone noise, and in the second case, a 100-300 Hz band noise was produced.

30-second sweeps were generated using three segments and compared to the most widely used exponential sweep. The exciting loudspeaker was a Yamaha SM151V for the first case and a Genelec 8050A for the second case. Recording was made using a Rion NL-32 sound level meter’s direct output digitized by an RME Fireface 800 sound module. Artificial noise was input in this system using a smaller Yamaha monitor loudspeaker in a physically different location in the reverberation room. The sweeps were faded in and out using a short, 5 ms Gaussian half-window. The impulse response was calculated using an uncompensated inverse filter based on the ideal sweep. The sampling frequency was 48 kHz.

A short portion of the observable noise (consisting of the equipment, room background and artificial noise) was first sampled and used as a reference to produce a close matching spectrum sweep. In this present approach matching was made manually but automatic matching may also be possible to implement in the near future.

In the first case, the generated sweeplet consisted of a sigmoid and two monomial sweeps with length ratios 16:8:4 from lower to higher frequency segments. Segment band limits were 30 to 990 Hz, 990 to 1800 Hz and 1800 to 24000 Hz. Generating parameters were for the sigmoid sweeplet: $d = \omega_2 + 10000$ and $c = 7$, for the first monomial segment $d = 1000 \cdot 2\pi$, $c = -1$ and $p = 3$ and for the second monomial segment $d = 2000 \cdot 2\pi$ with c and p the same as for the first segment.

In the second case, all segments contained two monomial and a red sweep. The first segment occupying 20 to 100 Hz was of log-shape $[d, c, p] = [\omega_2 - 10, -1, 3]$, the second between 100 and 300 Hz was linear $[d, c, p] = [\omega_2 + 10^7, 2, 3]$ and the third segment between 300 and 24000 Hz was a red sweep with $d = 0$. Focusing to such a low frequency may result in limited signal availablilty at very high frequencies if the signal length is not long enough. In this present case, the 30 second signal length shows this effect of time-windowing above 10 kHz (Fig. 8).

Results show lower noise level corresponding to SNR improvement in the desired frequency range (Fig. 9).

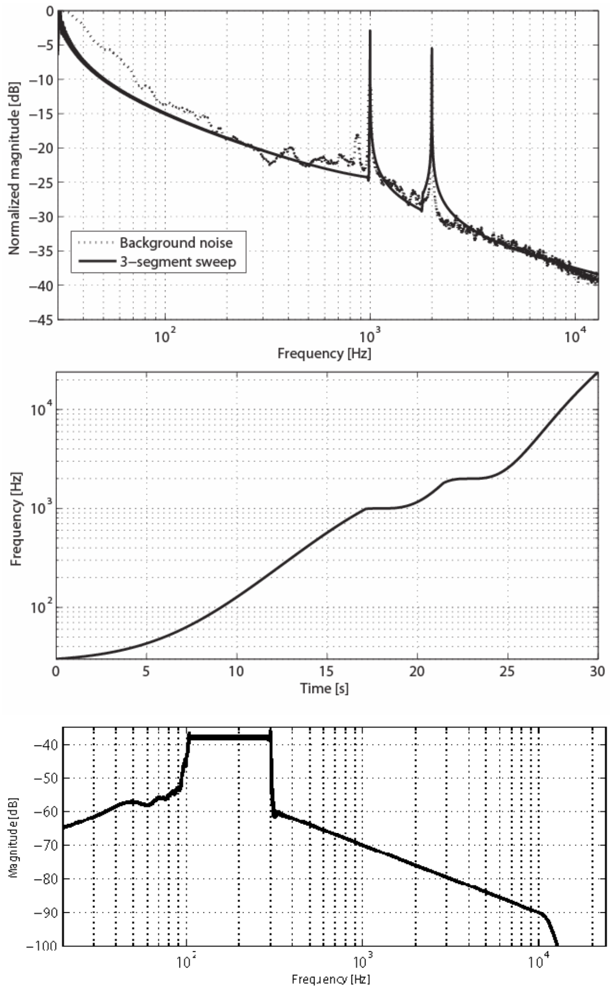

Figure 8. Overall magnitude spectrum and spectrogram of the 3-segment sine sweep optimized for the twin harmonic noise (top) and spectrum of the signal optimized for the 100-300 Hz band background noise. In the latter case, half-windowing attenuates the signal above 10 kHz.

CONCLUSIONS

In this paper, examples have been shown where currently available sweeps do not match the background noise observed in rooms therefore, particularly at lower frequencies, acceptable SNR is difficult to obtain.

Several new types of time-domain formulated sine sweeps were introduced and their use considered both theoretically and practically for room acoustic measurements.

The presently proposed sweeps can be effectively used to customize the overall frequency response of the excitation signal while maintaining the signal's perfect envelope, a result of their time-domain generation. Measurement examples demonstrate the applicability of the proposed method.

Since the results are available analytically, the proposed sweep signals can be implemented at the desired numeric accuracy. The formulas presented in this paper can be directly used to synthesize sweep signals with a desired magnitude spectrum.

REFERENCES

1 Y. Suzuki, F. Asano, H.Y. Kim, and T. Sone. An optimum computer generated pulse signal suitable for the measurement of very long impulse responses. *The Journal of the Acoustical Society of America*, **97**(2), 1119–1123, 1995.

2 M. Morise, T. Irino, H. Banno and H. Kawahara, Warped-TSP: An Acoustic Measurement Signal Robust against Background Noise and Harmonics Distortion, *Transactions of the Institute of Electronics, Information and Communication Engineers*, J89-A(1), pp. 7-14, 2006 (in Japanese)

3 A. J. Berkhout, D. De Vries and M. M. Boone. A new method to acquire impulse responses in concert halls. *The Journal of the Acoustical Society of America*, **68**(1), 179–183, 1980.

4 A. J. Berkhout, M. M Boone and C. Kesselman. Acoustic Impulse Response Measurement: A New Technique. *Journal of the Audio Engineering Society*, **32**, 740–746, 1984.

5 S. Muller and P. Massarani. Transfer-function measurement with sweeps. *Journal of the Audio Engineering Society*, **49**(6), 443–471, 2001.

6 N. Moriya and Y. Kaneda. Optimum signal for impulse response measurement that minimizes error caused by ambient noise. *Journal of the Acoustical Society of Japan*, **64**(12), 695–701, 2008 (in Japanese).

7 D. Griesinger. Beyond MLS-Occupied hall measurement with FFT techniques. *101st AES Convention Paper 4403*, Los Angeles, 1996. Audio Engineering Society, pp 1–23

8 A. Farina. Simultaneous measurement of impulse response and distortion with a swept-sine technique. *108th AES Convention Paper 5093*, 2000. Audio Engineering Society, pp 1–24

9 A. Farina. Advancements in impulse response measurements by sine sweeps. *122nd AES Convention Paper 7121*, Vienna, 2007. Audio Engineering Society, pp 5–8

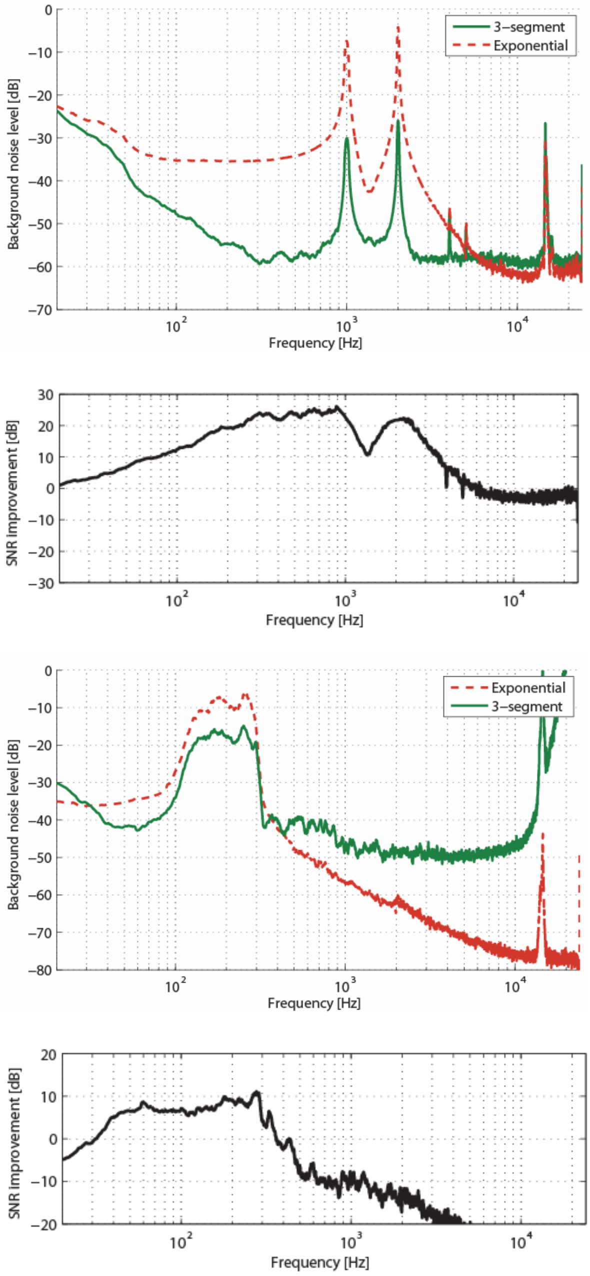

Figure 9. Relative background noise and SNR improvement in the impulse response in the presence of a two-harmonic noise in addition to the room noise (top two); and in the presence of additional 100-300 Hz band noise (bottom two). Optimization was achieved in these examples in the desired frequency range at the expense of SNR reduction in the other frequency ranges.